技 術 論 文

Chemical Kinetic Analysis with Two-Zone Model on Spark Knock Suppression Effects with Hydrogen Addition at Low and High Engine Speeds

**Jun Goto Yoshimitsu Kobashi Yoshito Ueno Gen Shibata
Hideyuki Ogawa Minoru Yamamoto**

要旨

　本研究では、異なる機関回転速度（低速ノックが生ずる2000rpm および高速ノックが生ずる4800rpm）における水素添加時の火花ノック抑制効果について検討を行った。実機実験の結果、水素添加は低速ノックに対しては強い抑制効果が得られる一方で、高速ノックに対しては効果が低下することが明らかとなった。その要因について二領域モデルによる化学動力学解析を行った結果、機関回転速度が2000rpm では未燃領域内において顕著な低温酸化反応が出現する二段の熱発生率となるのに対し、4800rpm では未燃混合気の低温滞留時間短縮に起因して低温酸化反応が出現しない一段の熱発生率となることがわかった。水素添加による火花ノック抑制メカニズムは主に水素の OH 消費にともなう低温酸化反応の抑制であり、低温酸化反応に強く依存した着火形態となる低速ノックに対しては強い抑制効果が得られる一方、これに強く依存しない着火形態となる高速ノックに対しては効果が低下することが明らかとなった。

Abstract

Spark knock suppression with hydrogen addition was investigated at two engine speeds (2000 rpm and 4800 rpm). The experimental results showed that the spark knock is strongly suppressed with increasing hydrogen fraction at 2000 rpm while the effect is much smaller at 4800 rpm. To explain these results, chemical kinetic analyses with a two-zone combustion model were performed. The calculated results showed that the heat release in the end gas zone rises in two stages with a remarkable appearance of low temperature oxidation (LTO) at 2000 rpm, while a single stage heat release without apparent LTO process is presented at 4800 rpm due to the shorter residence time in the low temperature region. The mechanism of the spark knock suppression with hydrogen addition can be explained by inhibition of the LTO reactions and H_2O_2 loop reactions by the OH radical consuming reaction with hydrogen, leading to a reduction in the heat release from hydrocarbon fuel at the initial stage of the ignition process. However, the OH radical is simultaneously produced from H radical with hydrogen addition at the later stage of the ignition process. The reduction in the heat release with hydrogen addition can only be obtained at the initial stage of the ignition process, and the differences in spark knock suppression with hydrogen addition under low and high engine speeds are due to absence or appearance of LTO at the initial stage of the ignition process.

1 INTRODUCTION

In spark ignition engines, a large exhaust loss is one of the primary issues preventing improvements in thermal efficiency. The exhaust loss is dependent on the specific heat ratio of the in-cylinder gas, the compression ratio, the combustion phase and the combustion period as detailed in Figure 1. Among these factors, the compression ratio and the combustion phase are particularly limited by spark knock.

Spark knock is known as abnormal combustion induced by the self-ignition in the end gas mixture[1]-[7]. Spark knock generally occurs at low engine speeds and tends to be suppressed with increasing engine speed due to the shortened high temperature residence time of the end gas mixture. However, further increase in the engine speed may also cause the spark knock phenomena called "high-speed knock" distinguishing it from "low-speed knock"[8].

As a way to avoid the spark knock, the utilization of hydrogen as an additive fuel has attracted attention. Hydrogen is known as an alternative fuel produced from renewable energy, and also can be produced on-board via fuel reforming. The reformed exhaust gas recirculation (REGR)[9]-[12] can reform hydrocarbon fuels into hydrogen, carbon monoxide, and methane with a reformer catalyst equipped in the path of the exhaust gas recirculation (EGR). The REGR has the potential to suppress the spark knock with the chemical effects of hydrogen as well as with EGR[13]-[19]. Additionally, as the reforming reactions are endothermic, the exhaust heat can be regenerated to the energy input[10]. The spark knock suppression with hydrogen addition has been widely investigated in the previous studies[20]-[30]. Naruke et al. showed that the hydrogen addition extended the knock limit at the engine speed of 2000 rpm under lean conditions[26]. Topinka et al. demonstrated that the required octane number of the primary reference fuel (PRF) to avoid spark knock can be decreased with increasing the hydrogen concentration at 1500 rpm under lean conditions[27]. Ashida et al. demonstrated that the spark knock resistance improves with reformate hydrogen at an engine speed of 1200 rpm under stoichiometric conditions[28]. Gerty and Heywood investigated the effect of simulated fuel reformate (a mixture of hydrogen, carbon monoxide, and nitrogen) on the spark timing at the knock limit for a variety of fuels at 1500 rpm under lean conditions and showed that the required combustion retardation to avoid knock can be decreased with reformate addition for PRFs and TRFs[29]. Shinagawa et al. investigated the effect of hydrogen addition at 1600 rpm under rich conditions and elucidated that the spark knock suppression with hydrogen addition is obtained with the inhibition of fuel

decomposition and hydroxyl radical production[30].

As described above, there are many reports of the influence of hydrogen addition on knocking characteristics at various conditions. However, most of the investigations were focused on the low-speed knock and the effects on the high-speed knock have not been clarified.

The previous studies have suggested that the phenomenon of the high-speed knock is different from that of the low-speed knock. Spicher et al. showed that the knock intensity at high engine speeds has higher sensitivity to spark ignition advance than at low engine speeds[31]. Iijima et al. visualized the combustion with spark knock over a wide range of engine speeds and revealed that the combustion proceeds at supersonic speed in the high-speed region, proposing that the phenomenon corresponds to a "developing detonation" extending to the strong knock events[32]. Goto et al. suggested that the spark knock at high engine speeds has a smaller dependence of the low temperature oxidation (LTO) on the ignition process as the end gas mixture has the shorter residence time in the low temperature region[33]. However, the detailed mechanism of the difference between low and high-speed knock is still not clearly explained. The ordinary way to avoid the high-speed knock was the fuel enrichment, but due to the upcoming enhanced emission regulations including Real Driving Emissions (RDE)[34], the fuel enrichment will not be acceptable in the future. Consequently, understanding the phenomenon and establishing new solutions for avoiding high-speed knock will be essential.

The objective of this study is to clarify the effect of hydrogen addition on the high-speed knock as well as on the low-speed knock and to obtain new insight into the difference between low and high-speed knock. The experiments were conducted at the two engine speeds of 2000 rpm and 4800 rpm and the crank angle at the spark knock onset changing with the quantity of hydrogen were assessed. Further, the chemical kinetic analyses with the two-zone model were performed to elucidate the influence of hydrogen addition on the

ignition process of the low and high-speed knock. Note that the motivation of this research is to improve the thermal efficiency with applying REGR. However, to understand the basic effects of hydrogen addition and to distinguish the effects of other reformed gas compositions, hydrogen was directly introduced to the intake pipe without REGR application in the present study.
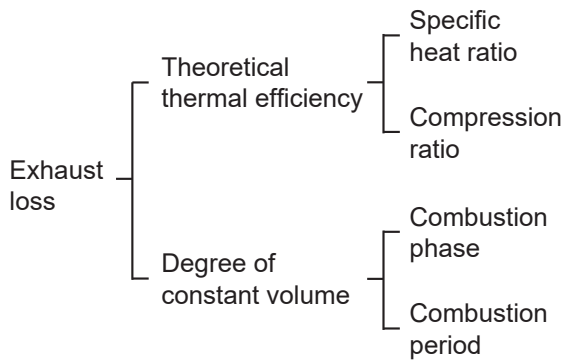

Fig. 1 Parameters related to the exhaust loss

2 EXPERIMENTAL SETUP

2-1. Engine Specifications and Experimental Procedures

The engine specifications are detailed in Table 1 and a schematic of the experimental system is shown in Figure 2. The experiments were conducted on a single cylinder, four-stroke, water cooled, naturally aspirated spark ignition engine. The main fuel was injected into the intake port and hydrogen was introduced into the intake pipe upstream of the throttle valve. The quantity of hydrogen was controlled with a mass flow controller (ALICAT, MCR-100SLPM-D), and the overall excess air ratio, λ, was maintained by adjusting the injection quantity of the main fuel based on the output of a universal exhaust gas oxygen (UEGO) air-fuel ratio sensor (Tsukasa Sokken, PLR-5) equipped in the exhaust pipe. The intake temperature was controlled with a heater in the intake pipe and the net indicated mean effective pressure, nIMEP, was maintained with a throttle valve. The in-cylinder pressure was measured with a piezoelectric pressure sensor (Kistler, 6053CC). The signal was amplified with a charge amplifier (Kistler,

5018A) and was recorded with a crank angle detector (ONO SOKKI, CP-5110A and CA-500A).

2-2. Experimental Conditions

The experimental conditions are detailed in Table 2. The engine operating conditions were set to the nIMEP of 900 kPa, intake temperature of 318 K, and λ of unity (1.0). The primary reference fuel with an octane number of 90, PRF90, a blend of iso-octane and n-heptane at 90:10 by volume, was used as the main fuel. The hydrogen addition fraction in the total lower heating value (LHV) was varied from 0 HV% to 15 HV%.

The onset of spark knock was determined by setting a specified limit to the band-pass filtered in-cylinder pressure profiles of 500 cycles over the frequency range of 9 to 18 kHz. The 50% mass burned crank angle, CA50, at the most advanced spark ignition timing without the occurrence of spark knock was defined as the knock limit.
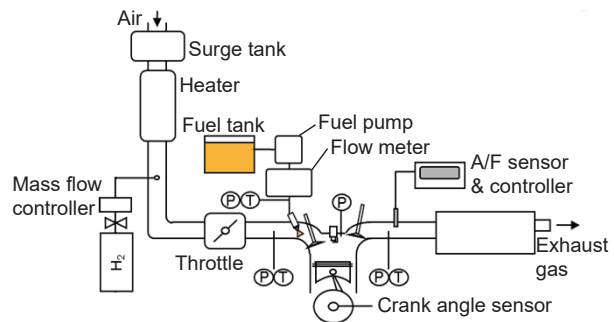

Fig. 2 Experimental arrangement

Table 1 Engine specifications

Number of cylinders [-]	1
Bore [mm] × Stroke [mm]	96 × 96
Displacement volume [cm^3]	695
Compression ratio	12.5:1
Fuel injection system	Port injection

Table 2 Experimental conditions

Engine speed [rpm]	2000, 4800
Net IMEP [kPa]	900
Intake air temperature [K]	318
EGR rate [%]	0
Main fuel	PRF90
H$_2$ additive fraction [HV%]	0 - 15
λ [-]	1

The engine speeds at the conditions of low and high-speed knock were determined with preliminary experiments. Figure 3 shows the relationship between the engine speeds and the CA50 at the knock limit. The tested gasoline here was a 50:50 blend of commercially available premium gasoline (research octane number, RON 100) and regular gasoline (RON 90). Increasing the engine speed from 2000 rpm, the spark knock tends to be suppressed and the CA50 at the knock limit temporarily advances below 3600 rpm. However, the further increase in the engine speed from 3600 rpm to 4800 rpm causes the spark knock to show up again and results in the retardation of the CA50 at the knock limit. From this result, the engine speeds were determined at 2000 rpm as the low-speed knock and at 4800 rpm as the high-speed knock.
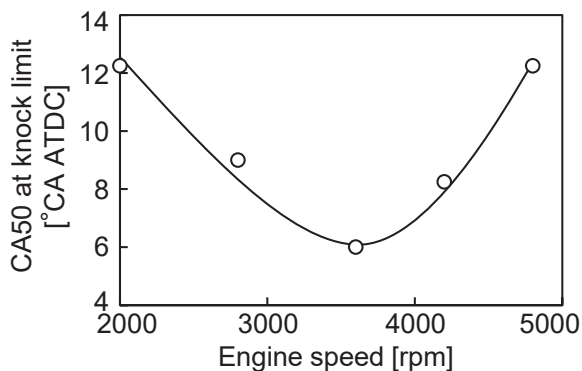

Fig. 3 Relationship between the engine speed and the CA50 at the knock limit

3 EXPERIMENTAL RESULTS

Figure 4 shows the effect of hydrogen addition on CA50 at the knock limit under the engine speeds of 2000 rpm and 4800 rpm. Increasing the hydrogen addition fraction, the CA50 at knock limit advances at both engine speeds. However, the advance of the knock limit is more significant at 2000 rpm than at 4800 rpm. This indicates that hydrogen addition strongly suppresses the low-speed knock, but the effect becomes smaller on the high-speed knock.
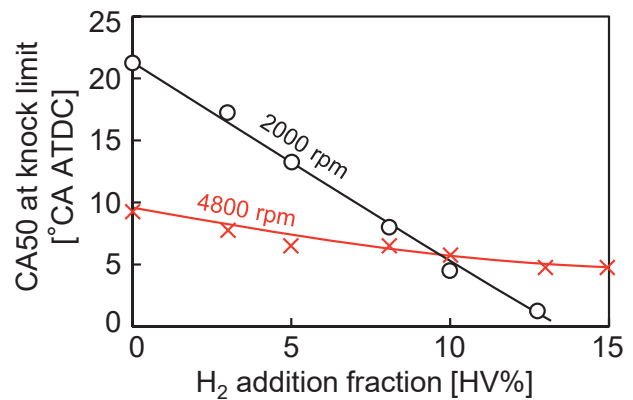

Fig. 4 Effect of hydrogen addition on the CA50 at the knock limit under engine speeds of 2000 rpm and 4800 rpm

A previous study by Goto et al. has investigated the effect of hydrogen addition on the ignition process with the chemical kinetic analyses at the initial temperatures of 700 K as a condition with a remarkable appearance of LTO and 1100 K as a condition skipping the LTO process under constant volume and adiabatic conditions[33]. The results showed that hydrogen addition inhibits the LTO reactions and increases the ignition delay at low initial temperature, but rather promotes the temperature rise at the high temperature region resulting in no increase in the ignition delay at the condition without the appearance of LTO. This result suggests that the smaller knock suppression effect at higher engine speeds may be due to the smaller dependence of the LTO process on high-speed knock. In the present study, the chemical kinetic analysis with a two-zone combustion model was applied for the further investigation of hydrogen addition effects on low and high-speed knock under actual engine operating conditions including piston compression.

4 CALCULATION METHOD

4-1. Two-zone Combustion Model

In the two-zone combustion model, the combustion chamber is divided into unburned and burned zones as shown in Figure 5. The mass of the mixture moves from the unburned zone to the burned zone in proportion to the heat release rate with the flame propagation. There is a virtual flame surface with no volume between the two zones and the chemical species in the flame surface

moved from the unburned zone instantly reach chemical equilibrium before moving to the burned zone. The chemical reactions depending on the temperature and the pressure proceed in the unburned and burned zones. It is assumed that there is no heat transfer between the two zones and that the pressures in the two zones are equivalent.
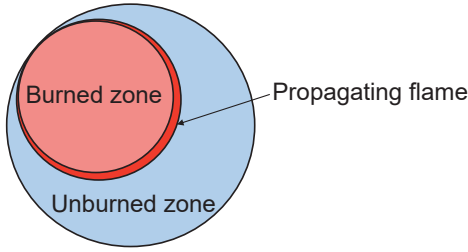

Fig. 5 Schematic of the two-zone combustion model

In this model, MATLAB (Math Works) was used as a platform, and Cantera[35] was used for the chemical kinetic calculations in the unburned and burned zones as well as for the chemical equilibrium calculations at the flame surface. A reduced reaction mechanism, SIP-Gr2.0 developed by Sakai and Miyoshi[36][37] was applied for the reaction model. The mechanism consists of the sub-mechanisms of a gasoline surrogate fuel (consisting of iso-octane, n-heptane, toluene, methylcyclohexane, and diisobutylene) and the base mechanism with the reactions of chemical species of zero to two carbon atoms, including hydrogen. The governing equations described below are formulated in the form of ordinary differential equations with respect to time, and the simultaneous equations were solved by the ODE solver of MATLAB.

4-1-1. Governing Equations

The governing equations for the unburned and burned zones can be described as follows.

Conservation of energy:

$$dU_u = d\left(m \sum_i^n h_i Y_i - pV \right)_u = \delta Q_{wall,u} - p\,dV_u - h_u dm_x \quad (1)$$

$$dU_b = d\left(m \sum_i^n h_i Y_i - pV \right)_b = \delta Q_{wall,b} - p\,dV_b + h_f dm_x \quad (2)$$

Conservation of chemical species:

$$d\left(m_u Y_{i_u} \right) = V_u W_{i_u} \dot{\omega}_{i_u} - Y_{i_f} dm_x \quad (3)$$

$$d\left(m_b Y_{i_b} \right) = V_b W_{i_b} \dot{\omega}_{i_b} + Y_{i_f} dm_x \quad (4)$$

Conservation of volume:

$$V = V_u + V_b \quad (5)$$

Equation of state:

$$p\,dV_u + V_u dp = R_u T_u dm_u + m_u R_u dT_u \quad (6)$$

$$p\,dV_b + V_b dp = R_b T_b dm_b + m_b R_b dT_b \quad (7)$$

Here, the subscript u indicates the unburned zone, b the burned zone, and f the flame surface. Y_i is the mass fraction of the chemical species i, dm_x the mass of the mixture moved from the unburned zone to the burned zone with the combustion, W_i the molecular weight of the chemical species i, and $\dot{\omega}_i$ the chemical reaction rate per unit time and unit volume. In equations (6) and (7), the derivative term of the gas constant is not considered, assuming that the change in the gas constant is sufficiently small and can be disregarded.

The first term on the right-hand side of equations (1) and (2) represents the heat transfer obtained from Woschni's equation[38] as follows:

$$\delta Q_{wall} = h_c A\left(T - T_{wall} \right) dt \quad (8)$$

$$h_c = C\,d^{m-1} p^m w^m T^{0.75-1.62m} \quad (9)$$

$$w = C_1 S_p + C_2 \frac{V_d T_r}{p_r V_r}\left(p - p_m \right) \quad (10)$$

Here, h_c is the heat transfer coefficient, T the gas temperature in the combustion chamber, T_{wall} the wall temperature of each part of the combustion chamber, and A the area. In this model, the heat transfers from the piston, the cylinder head, and the cylinder liner have been taken into consideration. The notation w is the representative velocity and corresponds to the average gas velocity in the cylinder. S_p is the average piston speed, and V_d is the displacement volume. T_r, p_r, and V_r are the temperature, pressure, and volume of the working gas at a specific timing, respectively, and the intake valve closing (IVC) timing was applied as the initial condition. The experimental constants C_1 was set at 2.28, and C_2 at zero before the spark ignition and at 3.24×10^{-3} after the spark ignition.

In the present study, the initial conditions described later were obtained by the one-dimensional engine modeling and simulation tool, GT-POWER (Gamma Technologies) and equation (9) was replaced as follows to be equalized with the analysis conditions of GT-POWER.

$$h_c = 3.01426 C_3 d^{-0.2} p^{0.8} w^{0.8} T^{-0.5} \tag{11}$$

A fitting parameter C_3 was set at 1.3, applied from the experimental results of the heat loss over a wide range of engine speeds. The cylinder diameter was used as a representative length d.

4-1-2. Simultaneous Ordinary Differential Equations

The ordinary differential equations of each physical quantity derived from the above governing equations can be described as follows.

Differentiation of pressure:

$$dp = \left(V - \frac{R_b V_b}{c_{p,b}} - \frac{R_u V_u}{c_{p,u}} \right)^{-1} \left[-p dV + \frac{R_b \cdot \delta Q_{wall,b}}{c_{p,b}} + \frac{R_u \cdot \delta Q_{wall,u}}{c_{p,u}} \right.$$

$$+ \left\{ R_b T_b - R_u T_u + \frac{R_b}{c_{p,b}} \sum_i^n Y_{if} \left(h_{if} - h_{ib} \right) \right\} dm_x$$

$$\left. - \frac{R_b}{c_{p,b}} V_b \sum h_{i_b} W_{i_b} \dot{\omega}_{i_b} - \frac{R_u}{c_{p,u}} V_u \sum h_{i_u} W_{i_u} \dot{\omega}_{i_u} \right] \tag{12}$$

Differentiation of temperature:

$$dT_u = \frac{\left(\delta Q_{wall,u} + V_u dp - V_u \sum h_{i_u} W_{i_u} \dot{\omega}_{i_u} \right)}{\left(m_u c_{p,u} \right)} \tag{13}$$

$$dT_b = \left[\delta Q_{wall,b} + V_b dp - V_b \sum h_{i_b} W_{i_b} \dot{\omega}_{i_b} \right.$$

$$\left. + dm_x \sum Y_{i_f} \left(h_{i_f} - h_{i_b} \right) \right] \left(m_b c_{p,b} \right)^{-1} \tag{14}$$

Differentiation of volume:

$$dV_u = \frac{R T_u dm_u + m_u R dT_u - V dp}{p} \tag{15}$$

$$dV_b = dV - dV_u \tag{16}$$

The simultaneous ordinary differential adding the chemical species conservation equations (3) and (4) to the above are solved in this model.

4-1-3. Heat Release Rates

The heat release rate with the flame propagation was obtained by approximating the composition of two Wiebe functions.

$$\frac{dQ}{d\theta} = a Q_0 Q_{mult1} \frac{m_1 + 1}{\theta_{z1}} \left(\frac{\theta}{\theta_{z1}} \right)^{m_1} \exp \left\{ -a \left(\frac{\theta}{\theta_{z1}} \right)^{m_1 + 1} \right\}$$

$$+ a Q_0 Q_{mult2} \frac{m_2 + 1}{\theta_{z2}} \left(\frac{\theta}{\theta_{z2}} \right)^{m_2} \exp \left\{ -a \left(\frac{\theta}{\theta_{z2}} \right)^{m_2 + 1} \right\} \tag{17}$$

Here, Q_0 is the total heat release, and θ_z is the combustion period. The notations a and m are constants and were determined from the experimental results under the conditions without hydrogen addition at each engine speed. There is the following relationship between dm_x, the mass transferred from the unburned zone to the burned zone, and $dQ / d\theta$, the heat release rate.

$$\frac{dQ}{d\theta} = LHV \cdot \frac{dm_x}{d\theta} \tag{18}$$

where LHV is the lower heating value.

4-1-4. Validation of the Model

The parameters of the Wiebe function are determined based on the experimental results at the engine speeds of 2000 rpm and 4800 rpm and are detailed in Table 3, and the comparison of heat release rates obtained with the experiments and the approximated Wiebe function at each engine speed are shown in Figure 6. Here, the start of combustion (where the heat release starts) was set at -9°CA ATDC for 2000 rpm and -19°CA ATDC for 4800 rpm, and hydrogen was not added at these engine speeds. Although there is a slight difference in the late combustion period, the approximated Wiebe function sufficiently reproduces the experimental results.

Table 3 Parameters of the Wiebe function

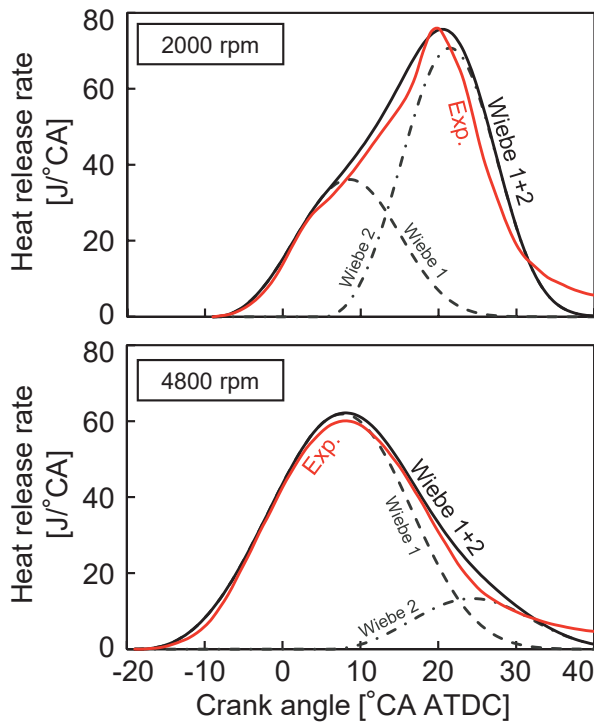| Engine speed [rpm]	2000	4800
a	6.9	
m_1/m_2	2.2/2.3	2.5/2.0
Q_{mult1}/Q_{mult2}	0.36/0.64	0.85/0.15
θ_{z1}/θ_{z2} (θ_{ztotal})	36.0/33.0 (47.0)	51.0/40.0 (65.0)

Fig. 6 Plots of the heat release rate obtained by the experiments and the approximated Wiebe function
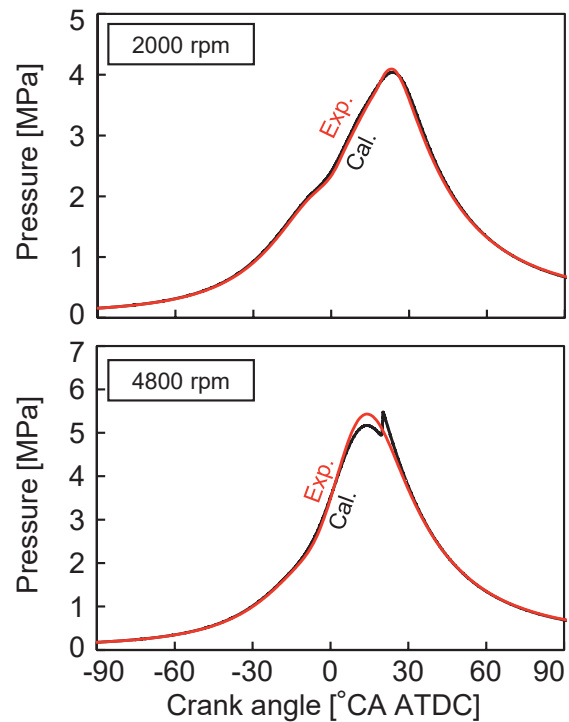

Fig. 7 Plots of the in-cylinder pressure obtained by the experiments and the two-zone combustion model

Figure 7 shows the comparison of in-cylinder pressure obtained by the experiment and the calculation of the two-zone combustion model with the parameters of the Wiebe function shown in Table 3. The calculation results of the two-zone combustion model can well reproduce the experimental results at both engine speeds. Here, the rapid pressure rise in the calculation result at 4800 rpm is caused by the autoignition in the unburned zone. Note that the experimental results are the ensemble average of 500 cycles and there is no pressure oscillation caused by spark knock.

4-2. Calculation Conditions

The calculation conditions are detailed in Table 4. The engine speeds were set at 2000 rpm and 4800 rpm. In addition to PRF90 and real hydrogen, virtual inert-hydrogen with the same thermodynamic properties as the real hydrogen without contributions from any chemical reaction[39] was applied to distinguish the effects of dilution and chemical reactions of hydrogen addition. The additive fraction of hydrogen or inert-hydrogen was set to 12.8 HV%, and λ to unity with adjustments to the mole fraction of the mixture. As the purpose of this study is to clarify the effect of hydrogen addition on low and high-speed knock from the point of view in chemical kinetics, the same heat release rates, the combustion start timings, and the initial conditions were applied both with and without hydrogen addition at each engine speed to eliminate the effects of differences in the pressure and temperature changes. Note that the difference is sufficiently small for the results not to change whether with or without considering the difference. The values of Table 3 were used for the parameters of the Wiebe functions, and the combustion start timings were determined as the points where the sufficiently large

spark knock occurs under the conditions with hydrogen addition at each engine speed. As the initial conditions, the in-cylinder pressure, the temperature, and the residual gas ratio at the IVC timing were calculated with GT-POWER with the Three Pressure Analysis (TPA) method. The TPA method is a non-predictive analysis to calculate the parameters which are difficult to measure directly such as the above-mentioned initial conditions by applying the measured intake, exhaust, and in-cylinder pressures referenced to the crank angle as the boundary conditions. The initial conditions were calculated after fitting the model with the measured in-cylinder pressure by adjusting the pressure loss and heat transfer parameters at each part of the engine.

Table 4 Calculation conditions

Engine speed [rpm]	2000	4800
Main fuel	PRF90	
Additives	12.8 HV% of H_2, inert-H_2	
λ [–]	1	
Start of combustion [°CA ATDC]	–23	–27

5 CALCULATION RESULTS

5-1. Difference Between Low-speed Knock and High-speed Knock

Figure 8 shows the effects of hydrogen and inert-hydrogen addition on the in-cylinder pressure and the end gas temperature under the engine speeds of (a) 2000 rpm and (b) 4800 rpm calculated with the two-zone combustion model. The spark knock occurs at both engine speeds, and significant pressure and temperature rises can be observed due to the self-ignition in the end gas. With hydrogen addition, the start of spark knock is retarded, and the pressure rise is suppressed due to the reduction of end gas volume at the spark knock timing, showing spark knock suppression effect at both engine speeds. However, the effect at 4800 rpm with the high-speed knock is smaller than at 2000 rpm with the low-speed knock, indicating that the calculation results are qualitatively consistent with the experimental results.

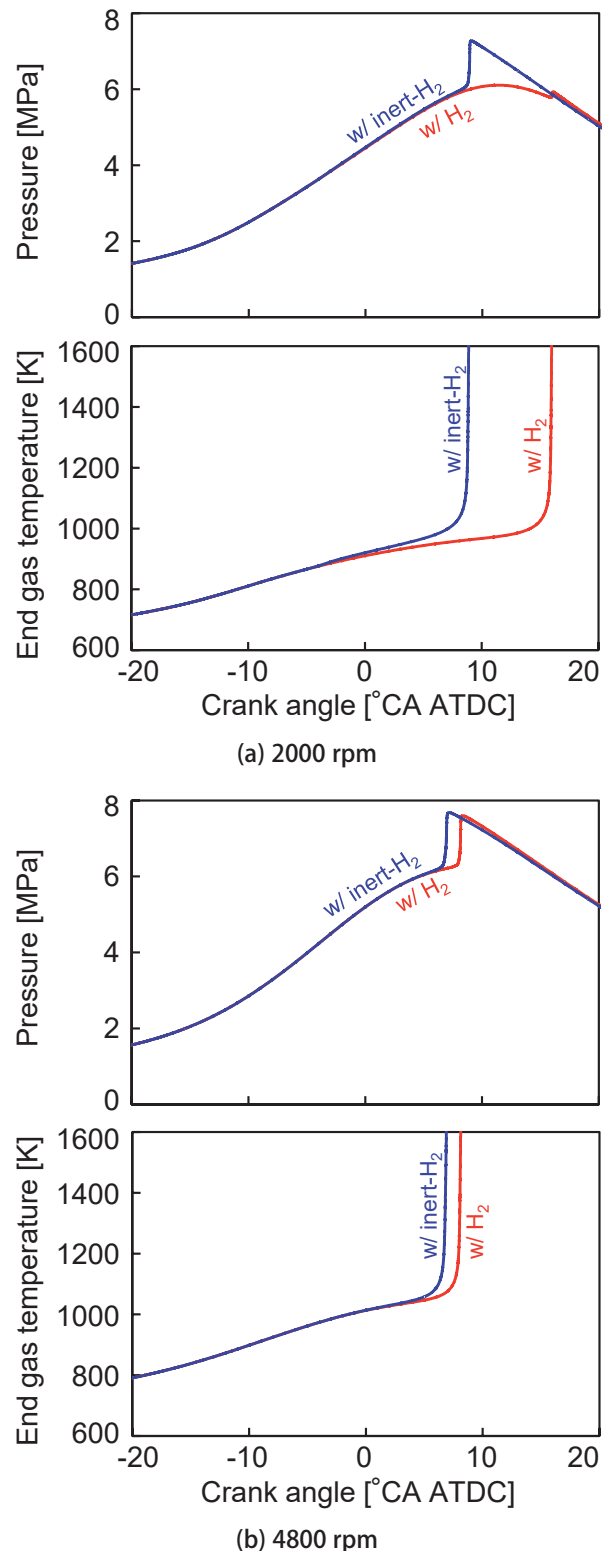
(a) 2000 rpm

(b) 4800 rpm

Fig. 8 Effects of hydrogen and inert-hydrogen addition on the in-cylinder pressure and the end gas temperature

Figure 9 shows the effects of hydrogen and inert-hydrogen addition on the heat release rate in the end gas under the engine speeds of (a) 2000 rpm and (b) 4800

rpm calculated with the two-zone combustion model. Under the condition with inert-hydrogen addition at 2000 rpm, a remarkable LTO appears between -5 to 0° CA ATDC, followed by a high temperature oxidation (HTO), and the heat is released in two stages. With hydrogen addition, LTO is suppressed and the appearance of HTO is significantly retarded. However, at 4800 rpm, the heat is released in a single stage without appearance of LTO even under the condition with inert-hydrogen addition, and hydrogen addition only slightly retards the appearance of HTO.

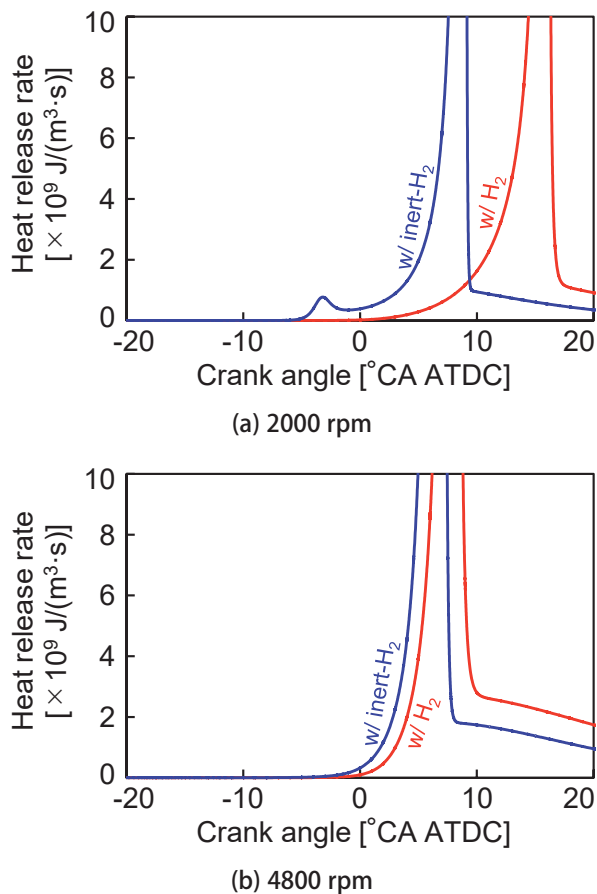(a) 2000 rpm

(b) 4800 rpm

Fig. 9 Effects of hydrogen and inert-hydrogen addition on the heat release rate in the end gas

Figure 10 shows the end gas temperature under the engine speeds of 2000 rpm and 4800 rpm, plotting the time after the IVC in the abscissa. The residence time in the temperature range of 600 to 900 K where LTO appears is longer at the low engine speed than at the high engine speed. This longer residence time at 2000 rpm leads to a larger dependence of LTO on the ignition process of the low-speed knock than of the high-speed knock at 4800 rpm, explaining the difference of the spark knock suppression effect with hydrogen addition between low and high engine speeds.
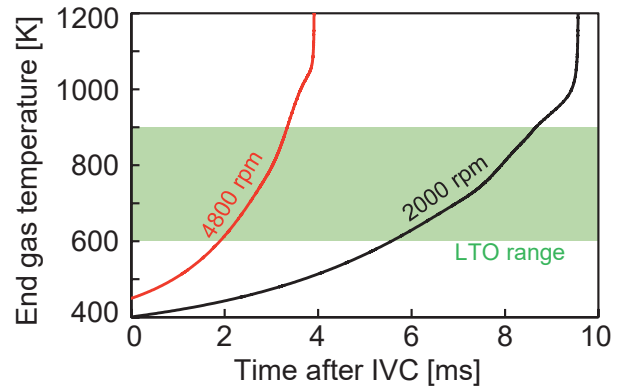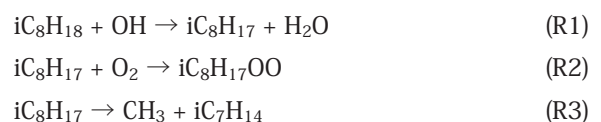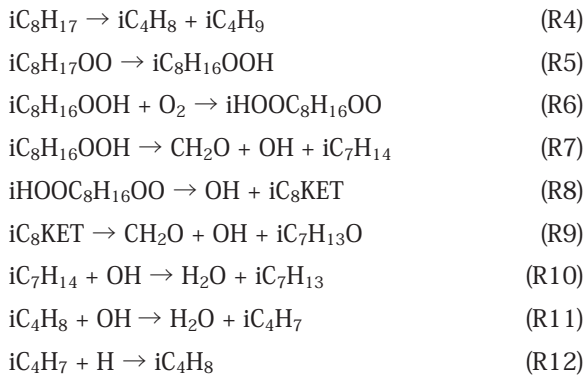

Fig. 10 End gas temperature vs time after IVC (with inert-hydrogen addition)
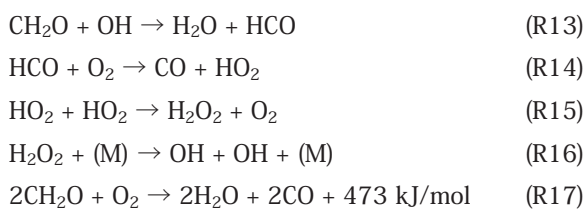
5-2. Effect of Hydrogen Addition on Low-speed Knock

Figure 11 shows the effects of hydrogen and inert-hydrogen addition on the heat release rates of representative elementary reactions in the end gas, and Figure 12 shows the concentrations of OH, iC_8H_{17}, CH_2O, H_2O_2, HO_2, and H with the additions of hydrogen and inert-hydrogen at the engine speed of 2000 rpm, plotting the temperature change with the reaction process in the abscissa. The fuel series is a group of reactions consisting of reactions (R1) to (R12), related to iso-octane, the major component of the main fuel. The oxidation process of iso-octane initiates from producing alkyl radicals by hydrogen abstraction with hydroxyl radicals (OH) (reaction (R1)). Under the low temperature conditions from 600 to 900 K, OH increases via the primary oxygen addition reaction, internal isomerization reaction, and secondary oxygen addition reaction (reactions (R2), (R5), (R6), (R8), and (R9)). The series of these processes is called "RO_2 chemistry"[40] and activates the reactions in the system. In addition, as the reactions (R1), (R2), and (R8) are exothermic, a heat release occurs as LTO in the above temperature range.

$$iC_8H_{18} + OH \rightarrow iC_8H_{17} + H_2O \qquad \text{(R1)}$$

$$iC_8H_{17} + O_2 \rightarrow iC_8H_{17}OO \qquad \text{(R2)}$$

$$iC_8H_{17} \rightarrow CH_3 + iC_7H_{14} \qquad \text{(R3)}$$

$$iC_8H_{17} \rightarrow iC_4H_8 + iC_4H_9 \quad (R4)$$

$$iC_8H_{17}OO \rightarrow iC_8H_{16}OOH \quad (R5)$$

$$iC_8H_{16}OOH + O_2 \rightarrow iHOOC_8H_{16}OO \quad (R6)$$

$$iC_8H_{16}OOH \rightarrow CH_2O + OH + iC_7H_{14} \quad (R7)$$

$$iHOOC_8H_{16}OO \rightarrow OH + iC_8KET \quad (R8)$$

$$iC_8KET \rightarrow CH_2O + OH + iC_7H_{13}O \quad (R9)$$

$$iC_7H_{14} + OH \rightarrow H_2O + iC_7H_{13} \quad (R10)$$

$$iC_4H_8 + OH \rightarrow H_2O + iC_4H_7 \quad (R11)$$

$$iC_4H_7 + H \rightarrow iC_4H_8 \quad (R12)$$

With the progress of the reactions, the main route of OH consumption shifts from reaction (R1) to (R13) due to the decrease in fuel and the increase in formaldehyde (CH_2O). This results in the degeneration of LTO, and the reaction system moves to the thermal ignition preparation period. In this period, the reaction with hydrogen peroxide (H_2O_2) produced from CH_2O via reaction (R13) to (R16) promotes the OH production by the thermal decomposition. The elementary reaction group consisting of reactions (R13) to (R16) is called the "H_2O_2 loop"[41][42]. The overall reaction of the H_2O_2 loop is exothermic as represented by reaction (R17), and greatly contributes to the heat release until the thermal ignition occurs.

$$CH_2O + OH \rightarrow H_2O + HCO \quad (R13)$$

$$HCO + O_2 \rightarrow CO + HO_2 \quad (R14)$$

$$HO_2 + HO_2 \rightarrow H_2O_2 + O_2 \quad (R15)$$

$$H_2O_2 + (M) \rightarrow OH + OH + (M) \quad (R16)$$

$$2CH_2O + O_2 \rightarrow 2H_2O + 2CO + 473 \text{ kJ/mol} \quad (R17)$$

The onset of thermal ignition can be defined as the point where the reaction rate of reaction (R18) exceeds that of reaction (R19)[43]. Reaction (R18) is a chain branching reaction which activates the reactions in the system increasing the number of radicals. However, the reaction itself is endothermic and does not contribute directly to the temperature rise. On the other hand, reaction (R19) is exothermic and considerably affects the temperature rise during the later stage of the thermal ignition preparation period.

$$H + O_2 \rightarrow O + OH \quad (R18)$$

$$H + O_2 + M \rightarrow HO_2 + M \quad (R19)$$

As shown in Figure 11 under the condition with inert-hydrogen addition, LTO appears at 850 to 900 K, followed by the gradually increase in the heat release with the H_2O_2 loop above 900 K. When the temperature reaches above 950 K with further increases, the heat release rate from reaction (R19) increases and the thermal ignition eventually occurs.

With hydrogen addition below 1000 K, the OH concentration is decreased due to the OH consumption by hydrogen as represented by reaction (R20), and due to the suppression of reaction (R1) around the start of iso-octane oxidation, the heat release from the subsequent LTO is reduced. The decrease in OH concentration also leads to the decrease in the CH_2O concentration, resulting in the reduction of the heat released from the H_2O_2 loop. However, the decrease in the OH concentration with hydrogen addition cannot be obtained above 1000 K with the increase in the H, HO_2, and H_2O_2 concentrations. This is due to the H produced by reaction (R20) eventually produces OH via the HO_2 and H_2O_2 by reactions (R19), (R15), and (R16). Thus, the heat release rate from the fuel series and H_2O_2 loop is less likely to be reduced, and the heat release rate from reaction (R19) increases. In addition, as reaction (R20) is exothermic, the activation of this reaction by hydrogen addition contributes to the temperature rise. The above results suggest that hydrogen addition has a large effect in reducing the heat release rate in the relatively low temperature region at the initial stage of the ignition process with LTO, but it rather promotes the temperature rise in the high temperature region with the progress of the reactions.

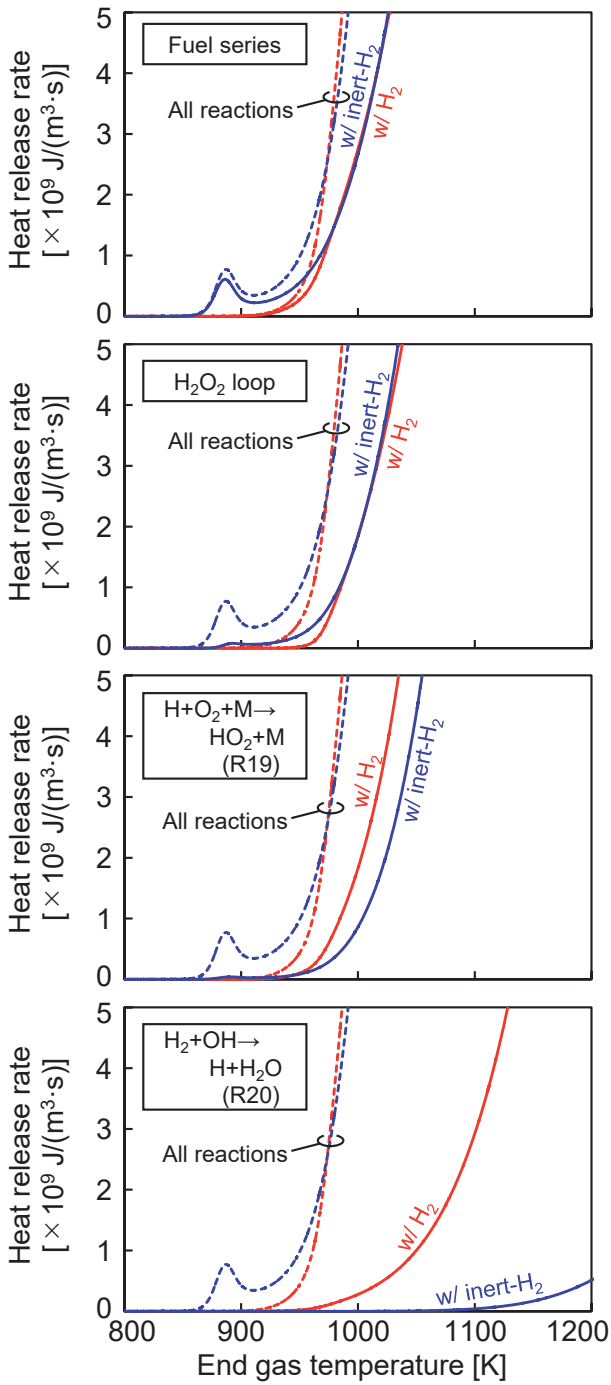$$H_2 + OH \rightarrow H + H_2O \quad (R20)$$

Fig. 11 Effects of hydrogen and inert-hydrogen addition on
the heat release rates of representative elementary
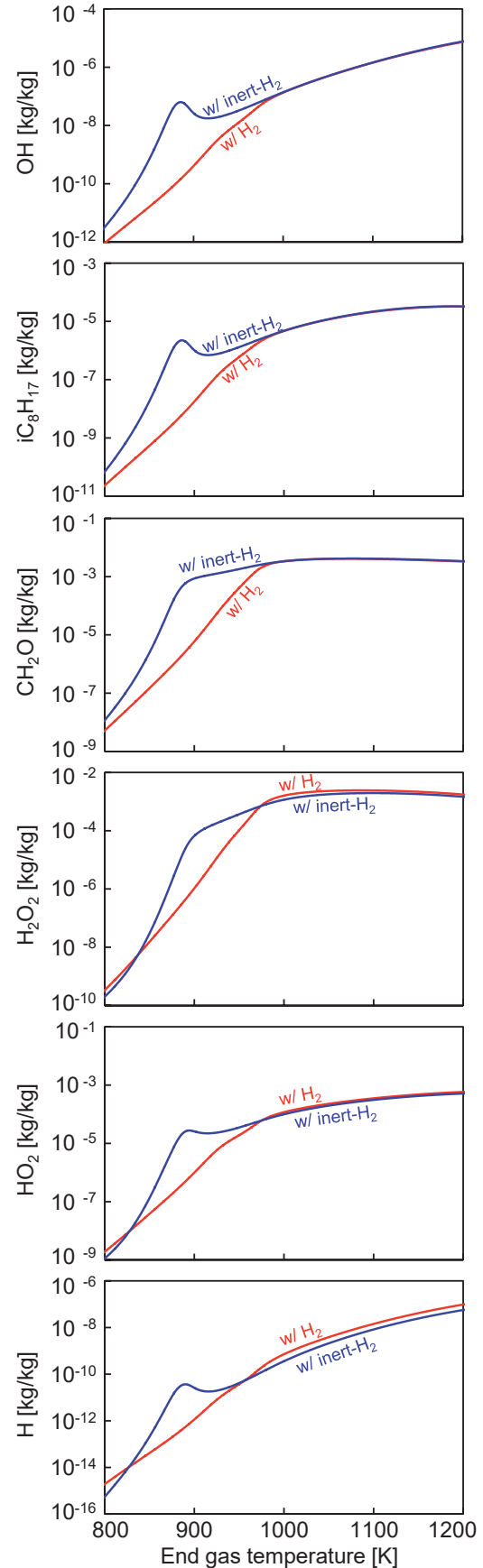reactions in the end gas (2000 rpm)

Fig. 12 Effects of hydrogen and inert-hydrogen addition
on the concentrations of chemical species (2000 rpm)

5-3. Effect of Hydrogen Addition on High-speed Knock

Figure 13 shows the heat release rates of representative elementary reactions in the end gas, and Figure 14 shows the concentrations of OH, iC_8H_{17}, CH_2O, H_2O_2, HO_2, and H with the additions of hydrogen and inert-hydrogen at the engine speed of 4800 rpm, plotting the temperature change with the reaction process in the abscissa. At 4800 rpm, the temperature rapidly increases before the progress of LTO reactions, resulting in the absence of any significant heat release below 1000 K. Although the start of iso-octane oxidation is reaction (R1) as the low-speed knock, the reactions in the high temperature region which alkyl radical decomposes to olefins and alkyl radicals with a small number of carbon atoms by reactions (R3) and (R4) becomes dominant over the heat release from the fuel series instead of LTO[44]. The decomposed species continue to the H_2O_2 loop by the subsequent reactions, and the temperature is raised together with reaction (R19) until the thermal ignition occurs.

With hydrogen addition, the OH concentration is decreased with hydrogen due to reaction (R20), leading to the suppression of reaction (R1) and the reduction of heat release from the fuel series and H_2O_2 loop as in the case of low-speed knock. However, since there is no appearance of LTO, the reduction in the heat release from the fuel series is smaller than in the case of low-speed knock. Further, due to the reactions onsetting at higher temperature, the heat release from reactions (R19) and (R20) activated by hydrogen addition increases at almost the same temperature as the fuel series and H_2O_2 loop. The effect of suppressing the temperature rise is cancelled, resulting in the small reduction effect in the overall heat release. The smaller effect of suppressing the high-speed knock with hydrogen addition can be explained by the absence of LTO at the initial stage of the ignition process with a shorter residence time in the low temperature region.
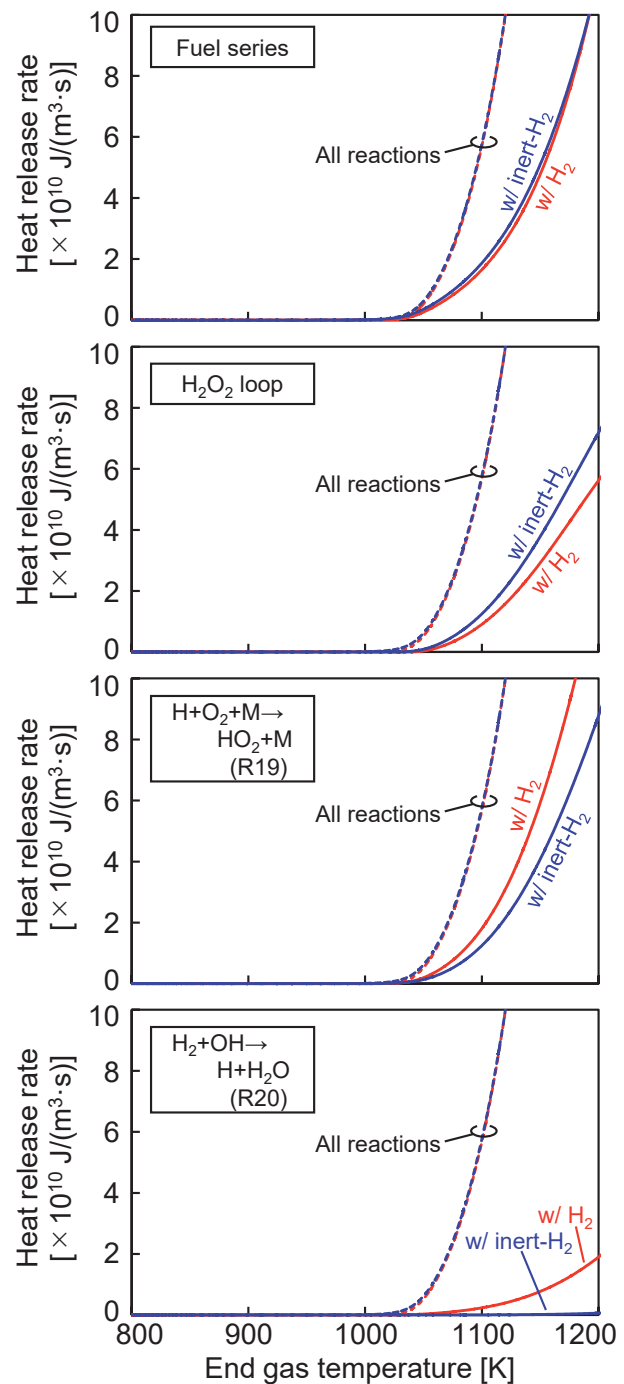

Fig. 13 Effects of hydrogen and inert-hydrogen addition on the heat release rates of representative elementary reactions in the end gas (4800 rpm)
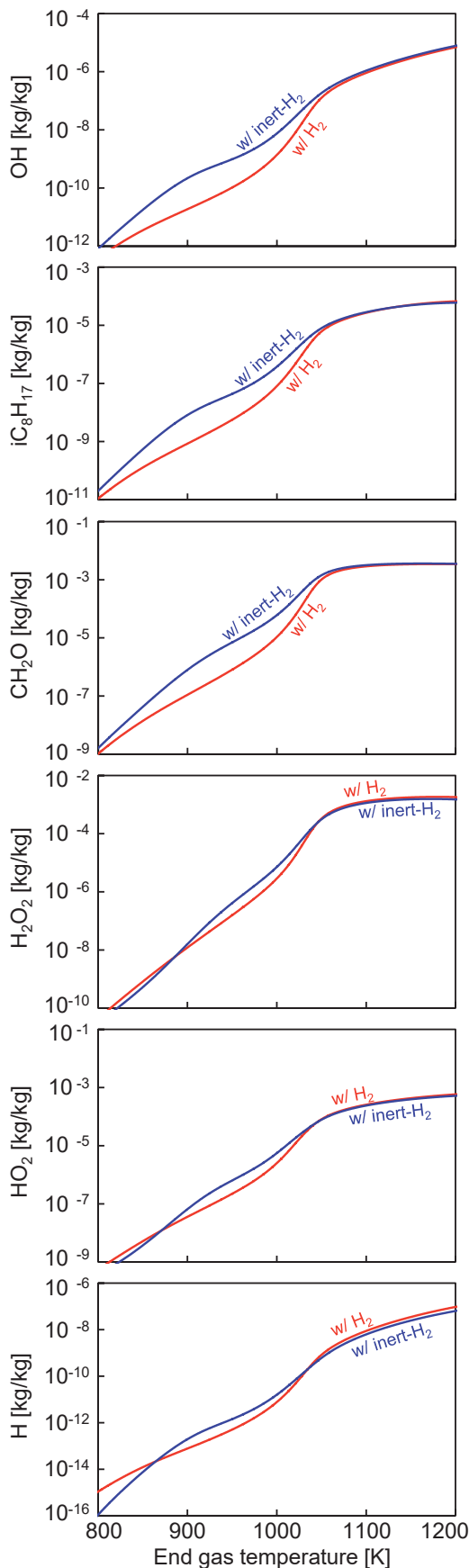
Fig. 14 Effects of hydrogen and inert-hydrogen addition on the concentrations of chemical species (4800 rpm)

6 CONCLUSIONS

In the present study, engine experiments and chemical kinetic analyses with a two-zone combustion model were performed to investigate the spark knock suppression effects of hydrogen addition at low and high engine speeds. The results may be summarized as follows:

1. Hydrogen addition can advance the combustion phase at knock limit at 2000 rpm, showing a large effect on suppressing the low-speed knock. However, the advance of the knock limit becomes smaller at 4800 rpm, and hydrogen addition is not effective for suppressing the high-speed knock.

2. In the calculation with the two-zone combustion model, the similar results as in the experiments were obtained, showing the smaller knock suppression with hydrogen addition at higher engine speeds.

3. At low engine speeds, the heat is released in two stages with a remarkable appearance of LTO, whereas at high engine speeds, the heat is released in a single stage due to the shorter residence time in the LTO temperature range.

4. The mechanism of spark knock suppression with hydrogen addition is the reduction in the heat release at the initial stage of the ignition process due to the OH consumption by hydrogen, and the temperature rise is promoted somewhat with hydrogen at the later stage of the ignition process under high temperatures.

5. The differences in the spark knock suppression with hydrogen addition under low and high engine speeds are due to the absence or presence of LTO at the initial stage of the ignition process.

REFERENCES

[1] G. Konig, C.G.W. Sheppard: "End-gas autoignition and knock in a spark ignition engine", SAE Paper 902135 (1990)

[2] U. Spicher, H. Kroger, J. Ganser: "Detection of knocking combustion using simultaneously high-speed schlieren cinematography and multi optical fiber technique", SAE Paper 912312 (1991)

[3] J. Pan, C.G.W. Sheppard: "A theoretical and experimental study of the modes of end-gas autoignition leading to knock in a S.I. engine", SAE Paper 942060 (1994)

[4] B. Stiebels, M. Schreiber, A. Sadat Sakak: "Development of a new measurement technique for the investigation of end-gas autoignition and engine knock", SAE Paper 960827 (1996)

[5] G. Topfer, J. Reissing, H.-J. Weimar, U. Spicher: "Optical Investigation of Knocking Location on S.I.-Engines with Direct-Injection", SAE Paper 2000-01-0252 (2000)

[6] U. Spicher, H.-P. Kollmeier: "Detection of flame propagation during knocking combustion by optical fiber diagnostics", SAE Paper 861532 (1986)

[7] J. B. Heywood: "Internal Combustion Engine Fundamentals", McGraw-Hill (1988)

[8] Y. Ohta: "INITATIONS OF ENGINE KNOCK: TRADITIONAL AND MODERN", Flame Structure, Vol. 2, pp. 372-375 (1991)

[9] S. Allenby, W.-C. Chang, A. Megaritis, M. L. Wysznski: "Hydrogen enrichment: A way to maintain combustion stability in a natural gas fuelled engine with exhaust gas recirculation, the potential of fuel reforming", Proceedings of the Institution of Mechanical Engineers, Vol. 215, Part D, pp. 405-418 (2001)

[10] S. Nagano, K. Yamazaki, Y. Mandokoro, I. Nakada, H. Yahagi: "Fuel Consumption Improvement by Engine EGR Reforming with Ethanol-Blended Gasoline Steam Reforming", Transactions of Society of Automotive Engineers of Japan, Vol. 43, No. 2, pp. 325-330, In Japanese (2012)

[11] K. Ashida, H. Maeda, T. Araki, M. Hoshino, K. Hiraya, M. Yasuoka: "Study of Hydrogen Additive High EGR Combustion for Gasoline Engine with Fuel Reformer", Transactions of Society of Automotive Engineers of Japan, Vol. 46, No. 4, pp. 743-748, In Japanese (2015)

[12] K. Hiraya, T. Araki, K. Ashida, A. Teraji: "A study of on-board EGR fuel reformer system on gasoline engine", Internal combustion engine symposium, No. 20196089, In Japanese (2019)

[13] I. Fukutani, E. Watanabe: "Knock Reduction of Spark-Ignition Engines by EGR", Transactions of the Japan Society of Mechanical Engineers, Part B, No. 52, Issue 474, pp. 991-996, In Japanese (1986)

[14] B. Grandin, H. E. Angstrom, P. Stalhammar, E. Olofsson: "Knock suppression in a turbocharged SI engine by using cooled EGR", SAE Paper 982476 (1998)

[15] T. Alger, B. Mangold, C. Roberts, J. Gingrich, "The Interaction of Fuel Anti-Knock Index and Cooled EGR on Engine Performance and Efficiency", SAE Paper 2012-01-1149 (2012)

[16] J. Bood, C. Brackmann, P. Bengtsson, A. Gogan, F. Mauss, B. Sunden: "Heat Release in the End-Gas Prior to Knock in Lean, Rich, and Stoichiometric Mixtures With and Without EGR", SAE Paper 2002-01-0239 (2002)

[17] S. Potteau, P. Lutz, S. Leroux, S. Moroz, E. Tomas: "Cooled EGR for a Turbo SI Engine to Reduce Knocking and Fuel Consumption", SAE Paper 2007-01-3978

[18] D. Parsons, S. Akehurst, C. Brace: "The potential of catalysed exhaust gas recirculation to improve high-load operation in spark ignition engines", International Journal of Engine Research, Vol. 16, Issue 4, pp. 1-14 (2015)

[19] E. Galloni, G. Fontana, R. Palmaccio: "Effects of exhaust gas recycle in a downsized gasoline engine", Applied Energy, Vo. 105, pp. 99-107 (2013)

[20] G. Lim, S. Lee, C. Park, Y. Choi, C. Kim: "Effects of compression ratio on performance and emission characteristics of heavy-duty SI engine fuelled with HCNG", International Journal of Hydrogen Energy, Vol. 38, pp. 4831-4838 (2013)

[21] S. Wang, C. Ji, B. Zhang, X. Liu: "Lean burn performance of a hydrogen-blended gasoline engine at the wide open throttle condition", Applied Energy, Vol. 136, pp. 43-50 (2014)

[22] J. Kim, K. M. Chun, S. Song, H.-K. Baek, S. W. Lee: "Hydrogen effects on the combustion stability, performance and emissions of a turbo gasoline direct injection engine in various air/fuel ratios", Applied Energy, Vol. 228, pp. 1353-1361 (2018)

[23] C. Park, Y. Choi, C. Kim, S. Oh, G. Lim, Y. Moriyoshi: "Performance and exhaust emission characteristics of a spark ignition engine using ethanol and ethanol-reformed gas", Fuel, Vol. 89, pp. 2118-2125 (2010)

[24] D. K. Marsh, A. K. Voice: "Quantification of knock benefits from reformate and cooled exhaust gas recirculation using a Livengood-Wu approach with detailed chemical kinetics", International Journal of Engine Research, Vo. 18, Issue 7, pp. 717-731 (2017)

[25] T. Han, G. Lavoie, M. Wooldridge, A. Boehman: "Effect

of Syngas(H2/CO) on SI Engine Knock under Boosted EGR and Lean Conditions", SAE International Journal of Engines, Vol. 10, No. 3 (2017)

[26] M. Naruke, K Morie, S. Sakaida, K. Tanaka, M. Konno: "Effects of hydrogen addition on engine performance in a spark ignition engine with a high compression ratio under lean burn conditions", International Journal of Hydrogen Energy, Vol. 44, pp. 15565-15574 (2019)

[27] J. A. Topinka, M. D. Gerty, J. B. Heywood, J. C. Keck: "Knock Behavior of a Lean-Burn, H2 and CO Enhanced, SI Gasoline Engine Concept", SAE Paper 2004-01-0975 (2004)

[28] K. Ashida, M. Hoshino, H. Maeda, T. Araki, K. Hiraya, M. Yasuoka: "Study of Reformate Hydrogen-Added Combustion in a Gasoline Engine", SAE Paper 2015-01-1952 (2015)

[29] M. D. Gerty, J. B. Heywood: "An Investigation of Gasoline Engine Knock Limited Performance and the Effects of Hydrogen Enhancement", SAE Paper 2006-01-0228 (2006)

[30] T. Shinagawa, T. Okumura, S. Furuno, K. Kim: "Effects of Hydrogen Addition to SI Engine on Knock Behavior", SAE Paper 2004-01-1851 (2004)

[31] U. Spicher, S. Palaveev: "Pre-Ignition and Knocking Combustion in Spark Ignition Engines with Direct Injection", JSAE Annual Congress Proceedings (Spring) No. 31-10, pp. 1-6 (2010)

[32] A. Iijima, S. Takahata, H. Kudo, K. Agui, M. Togawa, K. Shimizu et al.: "A Study of the Mechanism Causing Pressure Waves and Knock in an SI Engine under High-Speed and Supercharged Operation", International Journal of Automotive Engineering, Vol. 9, No. 1, pp. 23-30 (2018)

[33] J. Goto, Y. Kobashi, Y. Matsumura, G. Shibata, H. Ogawa, N. Kuragaki: "Spark Knock Suppression in Spark Ignition Engines with Hydrogen Addition under Low and High Engine Speeds", International Journal of Hydrogen Energy, Vol. 47, pp. 18169-18181 (2022)

[34] Delphi Technologies: "Worldwide emissions standards: Passenger cars and light duty vehicles 2020|21", https://www.delphi.com/sites/default/files/2020-04/DELPHI%20booklet%20emission%20passenger%20cars%202020%20online%20complet.pdf [accessed 25 April 2022]

[35] https://cantera.org/ [accessed 25 April 2022]

[36] Y. Sakai and A. Miyoshi: "Development of Reduced Chemical Kinetics Mechanism of Gasoline Surrogate Fuel", Internal combustion engine symposium, No. 20178019, In Japanese (2017)

[37] Y. Sakai, K. Hasegawa, A. Miyoshi: "Development of Reduced Chemical Kinetics Mechanism of Gasoline Surrogate Fuel with Oxygenated Compounds", Internal combustion engine symposium, No. 20183155, In Japanese (2018)

[38] G. Woschni, J. Fieger: "Experimental investigation of the heat transfer at normal and knocking combustion in spark ignition engines", Motortech.Z., Vol. 43, pp. 63-67 (1982)

[39] Y. Sakai, S. Ideue, H. Ando, K. Kuwahara: "Effects of Different Ignitability Fuel Addition on the Hydrocarbon Chemical Kinetic Mechanism", Transactions of Society of Automotive Engineers of Japan, Vol. 41, No. 3, pp. 697-702, In Japanese (2010)

[40] M. J. Pillimg: "Low-temperature Combustion and Autoignition", Elsevier (1997)

[41] H. Ando, Y. Sakai, K. Kuwahara: "Universal Rule of Hydrocarbon Oxidation", SAE Paper 2009-01-0948 (2009)

[42] K. Kuwahara and H. Ando: "Role of Heat Accumulation by Reaction Loop Initiated by H2O2 Decomposition for Thermal Ignition", SAE Paper 2007-01-0908 (2007)

[43] H. Ando and K. Kuwahara: "Difference of Reaction Schemes on Low Initial Temperature Conditions with LTO Reactions and High Initial Temperature Conditions Skipping Them", COMODIA2008 (2008)

[44] H. Ando, Y. Sakai, M. Syuu, K. Kuwahara: "Reaction Scheme of Various Hydrocarbon Fuels Under the Conditions Not Passing Through Low Temperature Oxidation Process", Transactions of Society of Automotive Engineers of Japan, Vol. 43, No. 2, pp. 311-317, In Japanese (2012)

DEFINITIONS/ABBREVIATIONS

EGR	exhaust gas recirculation
REGR	reformed exhaust gas recirculation
PRF	primary reference fuel
LTO	low temperature oxidation
HTO	high temperature oxidation
nIMEP	net indicated mean effective pressure
λ	excess air ratio
LHV	lower heating value
CA	crank angle
ATDC	after top dead center
CA50	50% mass burned crank angle
U	internal energy
m	mass
h	specific enthalpy
Y	mass fraction
p	pressure
p_m	motoring pressure
V	Volume
V_d	displacement volume
Q	heat release
Q_{wall}	heat transfer
W	molecular wight
$\dot{\omega}_i$	chemical reaction rate per unit time and unit volume
R	gas constant
T	temperature
T_{wall}	wall temperature
h_c	heat transfer coefficient
A	heat transfer area
d	representative length
w	representative velocity
S_p	average piston speed
C_p	specific heat at constant pressure

Subscripts

i	chemical species index
u	unburned zone
b	burned zone
f	flame surface
r	Representative

■著者

後藤 隼
Jun Goto
技術・研究本部
技術開発統括部
先進プロダクト開発部

小橋 好充
Yoshimitsu Kobashi
岡山大学
学術研究院環境生命
自然科学学域 准教授

上野 義人
Yoshito Ueno
北海道大学
大学院工学院
エネルギー環境システム専攻

柴田 元
Gen Shibata
北海道大学
大学院工学研究院
機械・宇宙航空工学部門 准教授

小川 英之
Hideyuki Ogawa
北海道大学
大学院工学研究院
機械・宇宙航空工学部門 特任教授

山本 稔
Minoru Yamamoto
技術・研究本部
技術開発統括部
先進プロダクト開発部